

Flow structure of knuckling effect in footballs

Short running head title: Football flow structure during knuckling

Takeshi Asai^a and Kyoji Kamemoto^b

^aCorresponding author

Institute of Health and Sports Science, B207

Comprehensive Human Sciences

University of Tsukuba

Tsukuba 305-8574, Japan

Tel. & Fax: (029) 853-2711

Email: asai@taiiku.tsukuba.ac.jp

^bDepartment of Engineering

Yokohama National University

Yokohama 240-8501, Japan

Tel.: 046-256-1207, Fax: 046-255-5137

Email: kamemoto@bg.mbn.or.jp

Abstract

The flight trajectory of a non-spinning or slow-spinning soccer ball might fluctuate in unpredictable ways, as for example, in the many free kicks of C. Ronaldo. Such anomalous horizontal shaking or rapid falling is termed the 'knuckling effect'. However, the aerodynamic properties and boundary-layer dynamics affecting a ball during the knuckling effect are not well understood. In this study, we analyse the characteristics of the vortex structure of a soccer ball subject to the knuckling effect (knuckleball), using high-speed video images and smoke-generating agents. Two high-speed video cameras were set at one side and in front of the ball trajectory between the ball position and the goal; further, photographs were taken at 1,000 fps and a resolution of 1024×512 pixels. Although in a previous study (Taneda, 1978), shedding of horseshoe vortices was observed for smooth spheres in the Reynolds number (Re) range of $3.8 \times 10^5 < \text{Re} < 10^6$, in the case of the soccer ball, the vortex structure, which consisted of distorted loop vortices, appeared in the wake behind the ball in the super-critical Re number region. Moreover, after the knuckleballs were airborne, large-scale undulations were observed in the vortex trail visualised with a smoke technique. On the other hand, aerodynamic forces acting on the ball were estimated from the data of the ball's flight trajectory, and a statistically high correlation ($r = 0.94, p < 0.01$) between the fluctuation frequency of the lift force and the undulation frequency of the vortex trail was shown to exist. This fact suggests that the phenomenon of large-scale undulations of the vortex trail is closely related to the cause of the unsteady aerodynamic forces acting on the knuckle ball.

Keywords: Visualization, Knuckling effect, Vortex, Ball, Soccer

1. Introduction

The flight trajectory of a non-spinning or slow-spinning soccer ball can fluctuate in unpredictable ways, as, for example, in the many free kicks of C. Ronaldo. Moreover, soccer balls often exhibit anomalous horizontal shaking or rapid falling, as a result of a phenomenon termed the ‘knuckling effect’ (Mehta, 1985).

Past research on knuckle balls has been performed predominantly in the context of baseball, with investigations into the effects of the ball’s flight speed, rotational velocity, rotational axis, and seams on air pressure and flight trajectory (Briggs, 1959; Adair, 1995; Watts and Bahill, 2000). In particular, Watts and Sawyer (1975) concluded that fluctuating lateral forces might be generated if a portion of the seam is located just at the point where boundary-layer separation occurs. However, the aerodynamic properties and boundary-layer dynamics of a ball subject to the knuckling effect (*knuckleball*) are not well understood.

In the case of the vortex structures of the flow around a smooth sphere, Achenbach (1974) showed that when the Reynolds number (Re) is 10^3 , complex vortex loops instead of an axisymmetric ring vortex structure are formed and when Re is 5×10^4 , the non-axisymmetric separation point tends to rotate. Taneda (1978), observed flows past a sphere for Re ’s ranging from 10^4 to 10^6 and reported the following characteristics of vortex structures in the wake flow: When Re ranges between 10^4 and 3.8×10^5 , the sphere wake exhibits a progressive wave motion in a plane containing the streamwise axis through the centre of the sphere. Further, the plane rotates slowly and irregularly about that axis. The wavelength is approximately 4.5 times the sphere diameter. For Re ’s ranging from 3.8×10^5 to 10^6 , the sphere wake forms a pair of streamwise line vortices at a short distance from the streamwise

axis. The vortex pair rotates slowly and randomly about that axis. Sakamoto & Haniu (1995) studied experimentally the vortex loop structure and vortex-shedding process when Re is greater than 8.0×10^2 in subcritical range. Furthermore, by using large eddy simulations at Re of 10^4 , Yun et al. (2003) showed that the large-scale structure of the wake forms a spiral flow pattern. However, the details of vortex structure of a smooth sphere at higher Re 's are still unclear. Nevertheless, to understand the unsteady phenomena observed in the free flight of a soccer ball, it is important to study the effects of vortex structures at high Re 's on flight features. Bearman & Harvey (1976) suggested that the vortex structure of a sports ball is closely related to its trajectory and dynamics, but the former in both the near-wake and the far-wake still remain to be investigated.

The fundamental aerodynamics of soccer balls have been studied previously by a group that included one of the present authors, using wind-tunnel experiments (Asai et al., 2007) in which the balls were fixed in the tunnel with a constant direction of flows. However, considering the knuckling effect of anomalous horizontal shaking or rapid falling in actual flight of a soccer ball, it seems that the aerodynamic characteristics of the flow around a ball in free flight might be different from those obtained from wind tunnel experiments, since the ball's motions of shaking and falling cause unsteady fluctuations in velocity and flow direction of the relative flow. Moreover, it may be possible that the wake structure and vortex-shedding characteristics in the state of free motion are interestingly related to the aerodynamic forces acting on a soccer ball in real flight. Therefore, to understand the phenomenon of the knuckling effect, it is necessary to perform experimental observation of flows

past a soccer ball by using flow visualisation techniques; it is also important to conduct unsteady-state analysis of the wake structures during real flights.

In this study, the vortex-shedding characteristics and far-wake structure behind a soccer ball in the state of knuckleball in actual flight were experimentally investigated by using high-speed video images and a smoke-generating agent.

2. Experiments

In the present study, the operation of experiments was set up outdoors and conducted in the following manner. A soccer ball (Europass; Adidas, 14 panels) was placed 25 m from and directly in front of a soccer goal (Figure 1). A subject kicked the ball towards the goal in such a manner that there were virtually no rotations, thereby resulting in a knuckleball (Figure 2). Each trial was performed under low wind conditions (<2.0 m/s). Kicks were delivered at a range of speeds that are typically experienced in real games. The trajectory of the ball was tracked by two high-speed (1000 fps) video cameras (resolution: 1024×1024 pixels) that were placed halfway between the ball position and goal, on either side of the expected ball trajectory, positioned to take pictures of both the top and side views. In the present study, only the pictures of trials of kicking with low spin rates (<12.56 rad/s) and clear demonstrations of the knuckling effect were used for the digital video analysis. Since the images of video pictures are usually warped due to optical strains caused by the camera lens, it is necessary to remove them to obtain proper positional coordinates in analysis. Hence, each video picture image was amended by using a compensation filter based on an affine transformation, in which the effectiveness and quality of the

image compensation were confirmed by comparing an original image with a revised one.

The three-dimensional coordinates of the instantaneous position of a ball were estimated from the side view and top view images. The data of calculated coordinates were processed by using a low-pass filter (LPF, 5-point moving average); furthermore, to reduce the influence of noise in the digitising process, the analysing frame rate of the video picture was reduced from 1000 fps to 100 fps. After data processing, instantaneous velocity and acceleration of the ball were calculated, using first- and second-order numerical differentiation. The instantaneous lift and side forces acting on the ball were calculated from the estimated instantaneous acceleration and mass of the ball (mass=0.43 kg). In addition, the frequency of fluctuation of the lift and side forces was calculated for the time period between a pair of neighbouring peak points of the curves of the lift and side forces versus time.

Flow visualisation around a ball in flight was achieved by using a smoke technique, using titanium tetrachloride as the smoke-generating agent. Each soccer ball was brush painted with the smoke generating agent and then kicked towards the goal. Finally, the ball was collected and cleaned. The nature of airflow around the ball was revealed by the generated white smoke in photographs obtained by high-speed video cameras.

On the other hand, as there was an observed undulatory structure in the images of flow patterns of the far-wake, the frequency of appearance of the large-scale undulation was calculated by comparing the visualised flow pattern with the trace of ball's trajectory and by assuming that the convective velocity of the smoke was negligibly small in comparison with the speed of ball.

3. Results and Discussion

An example of the trajectory of a knuckleball, obtained from our experiments, is shown in Figure 3. It can be clearly observed that fluctuations of trajectory in both lateral and vertical displacements exist. It is known from this figure that the amplitude of fluctuating distances becomes large up to the magnitude of approximately ± 0.05 m in this case, and similar tendencies have been confirmed in other cases.

As shown in Figure 4, the visualized flow patterns reveal that the aerodynamic features of the wake flow past a knuckleball in flight are slightly different from those usually observed behind a stationary ball in a uniform flow. Interestingly, a unique and undulatory structure of vortical flow in the far-wake region is observed in the visualised flow patterns. Furthermore, although the ball is flying with very little rotational motion in the experiments, the direction of flow of separated shear layers just behind the ball tends to deflect from its flight direction at this moment, and it forms a distorted vortex trail in the near-wake region. It is worthy to note that the whole wake structure, consisting of a row of vortex clouds, is not similar to the characteristics of either the subcritical regime or the supercritical regime on a smooth sphere (Taneda, 1978; Achenbach, 1972). The Reynolds number Re of the flow shown in Figure 4 was approximately 3.8×10^5 ; thus considering that the critical Reynolds number for a soccer ball is around 3.0×10^5 (Asai et al., 2007), the flow is thought to be in the supercritical regime. However, the above mentioned large-scale vortex structure is different from that observed in the supercritical regime ($Re = 6.0 \times 10^5$) of a smooth sphere (Taneda, 1978). This dissimilarity of flow characteristics might be attributed to the difference in the critical Re , based on the differences in the

ball panel shapes and surface roughness, but further investigation will be necessary to clarify the effects of surface conditions of a ball on variation of the critical Reynolds number.

In order to understand the aspects of the near wake of a ball exhibiting large-scale undulations, zoomed-in video images were used, as shown in Figure 5, and it was interestingly observed that the position of the separation point of the boundary layer seems to have moved further downstream than that of the subcritical region.

Therefore, it appears that the ball was flying at Reynolds numbers in the supercritical region. On the other hand, the vortex structure of the deflecting wake flow in the vicinity of the ball was sometimes similar to a hairpin vortex or a horseshoe vortex, as shown in Figure 6; this type of structure, however, was very unstable as shown in Figure 5. Although the mechanism of the phenomenon of the wake instability observed just behind the rear surface of the ball is not clear, it is possible to surmise that the phenomenon of unsteady deflection of the vortex trail suggests the onset of fluctuation of aerodynamic forces acting on the ball in flight, which results in the formation of the undulatory structure of the far wake. Fluctuating lateral forces acting on a knuckle ball in baseball are highly dependent upon the effects of the ball's seam, but as the seams on a soccer ball are relatively small, one may expect a proportionately reduced effect.

In Figure 7, the time history of vertical force (lift force) acting on the ball calculated from the data of its displacements is shown together with the flight trajectory of the knuckleball, in which the side viewed picture of the undulatory flow pattern of the wake is superposed. It is known from this figure that although the large-scale undulation path of the wake (streak line) is different from that of the ball

trajectory (path line), the oscillation waveform of the vortex wake and the waveform of the vertical (lift) force are almost in an antiphase relation. This kind of relation between the flow pattern of the wake and the ball trajectory was clearly observed in other knuckleball tests.

As shown in Figure 8, a comparison of the frequency of the fluctuation of lift force with the frequency of the undulation period of the wake, indicates that both frequencies are closely related to each other with a statistically high correlation ($r = 0.94$, $p < 0.01$). There are numerous factors that affect the frequencies of fluctuating lateral forces that act on a thrown ball, such as vortex shedding, ball rotation, and seam effects, and these likely comprise an extremely large number of frequencies. In this experiment, however, we focused our investigation solely on the relationship between the frequency of the fluctuation in the lift and side forces and the frequency of the undulation period of the wake in the low frequency range, as these are the most predominant and the easiest to observe and measure.

In the case of a baseball, fluctuating lateral forces acting on a knuckle ball are highly dependent upon the effects of the ball's seam, and are greatly affected by the ball's rotation rate (Watts and Sawyer, 1975). The effects of rotation are likely to be comparatively small, however, for a slowly rotating soccer ball (Table 1). Therefore, it can be concluded that the large-scale vortex undulation phenomenon is caused by the unsteady characteristics of the lift and side forces acting on a knuckleball.

Although the mechanism of the appearance of the unsteadiness in aerodynamic forces is not clear, it seems that the instability of separation of boundary layers might be increased by the knuckling effect of the soccer ball. The results of the present experiments clearly suggests that the ball kicking technique, which controls the

generation of large-scale undulations in the vortex trail, determines whether a straight ball or a knuckleball is produced.

4. Conclusions

In this study, to analyse the knuckling effect of a soccer ball in actual flight, the characteristics of the unsteady wake structure were experimentally investigated by using high-speed video images and a smoke-generating agent. High-speed video camera images of an in-flight knuckleball revealed a slightly irregular vortex shedding in its path, as well as large-scale undulations in the vortex trail. The experimental data indicate that the frequency of fluctuation of lift and side forces and the frequency of wake oscillation are closely related to each other with a statistically high correlation ($r = 0.94$, $p < 0.01$). From these results, the present study concludes that the phenomenon of large-scale vortex undulation in the wake is caused by the unsteady characteristics of the lift and side forces acting on a knuckleball, which might be related with the extraordinary instability in the separation of boundary layers.

References

- Achenbach, E., 1972. Experiments on the flow past spheres at very high Reynolds numbers. *Journal of Fluid Mechanics*. 54, 565–575.
- Achenbach, E., 1974. Vortex shedding from sphere. *Journal of Fluid Mechanics*. 62, 209–221.
- Adair, R.K., 1995. The physics of baseball. *Physics Today*. 48, 26–31.
- Asai, T., Seo, K., Kobayashi, O., Sakashita, R., 2007. Fundamental aerodynamics of the soccer ball. *Sports Engineering*. 10(2), 101–109.
- Bearman, P.W., Harvey, J.K., 1976. Golf ball aerodynamics. *Aeronautical Quarterly*. 27, 112–122.
- Briggs, L.J., 1959, Effect of spin and speed on lateral deflection (curve) of a baseball and Magnus effect for smooth spheres. *American Journal of Physics*, 27, 589–596.
- Mehta, R.D., 1985. Aerodynamics of sports balls. *Annual Review of Fluid Mechanics*. 17, 151–189.
- Sakamoto, H., Haniu, H., 1995. The formation mechanics and shedding frequency of vortices from a sphere in uniform shear flow. *Journal of Fluid Mechanics*. 287, 151–171.
- Taneda, S., 1978. Visual observations of the flow past a sphere at Reynolds numbers between 10^4 and 10^6 . *Journal of Fluid Mechanics*. 85, 187–192.
- Watts, R.G., Bahill, A.T., 2000. *Keep Your Eye on the Ball, Curve Balls, Knuckleballs, and Fallacies of Baseball*, W.H. Freeman and Co., New York.
- Watts, R.G., Sawyer, E., 1975. Aerodynamics of knuckleball. *American Journal of Physics*. 43, 960–963.

Yun, G., Choi, H., Kim, D., 2003. Turbulent flow past a sphere at $Re=3700$ and 10^4 .
Physics of Fluids 6, 15–19.

Table and Figure Captions

Table 1. The frequency of the fluctuation of lift and side force, the frequency of wake oscillation (Vortex), and the rotation rate of the ball (Rotation).

Figure 1. A close up picture of the soccer ball used in this experiment.

Figure 2. Experimental set up. A soccer ball was placed directly in front at a distance of 25 m from a soccer goal. A subject kicked the ball such that it had virtually no rotation and produced a knuckleball.

Figure 3. Ball trajectory and ball velocity of knuckleball. Displacement of the ball from top view (a) that of side view (b) and ball velocity (c).

Figure 4. Large-scale undulations in vortex trail of knuckleball. The flow direction is from left to right. The initial ball velocity is 28 m/s. The top image (a) is the side view, and the bottom image (b) is the top view of the visualisation experiment obtained using high-speed video cameras (1000 fps).

Figure 5. Sequence of video images showing deflection stages in near-wake flow (side view: a, b, c) of knuckleball. The initial ball velocity is 24 m/s. The flow direction is from left to right. The time after impact progresses from (a) to (c), as shown below each image. The near-wake flow in the vicinity of the ball deviated asymmetrically in the flight direction in a manner that was related to the large-scale undulations of the vortex trail.

Figure 6. Vortex structure of deflecting wake flow appearing somewhat similar to distorted loop vortex or hairpin vortex. The initial ball velocity is 24 m/s for (a) and 25 m/s for (b).

Figure 7. Relationship between ball trajectory from the side view (a) and the top view (b) (digitising marker), vortex shedding (flow direction is from right to left), and vertical and lateral acting force (c) on knuckleball. The time step of the digitizing marker indicating the centre of the ball is 10 ms.

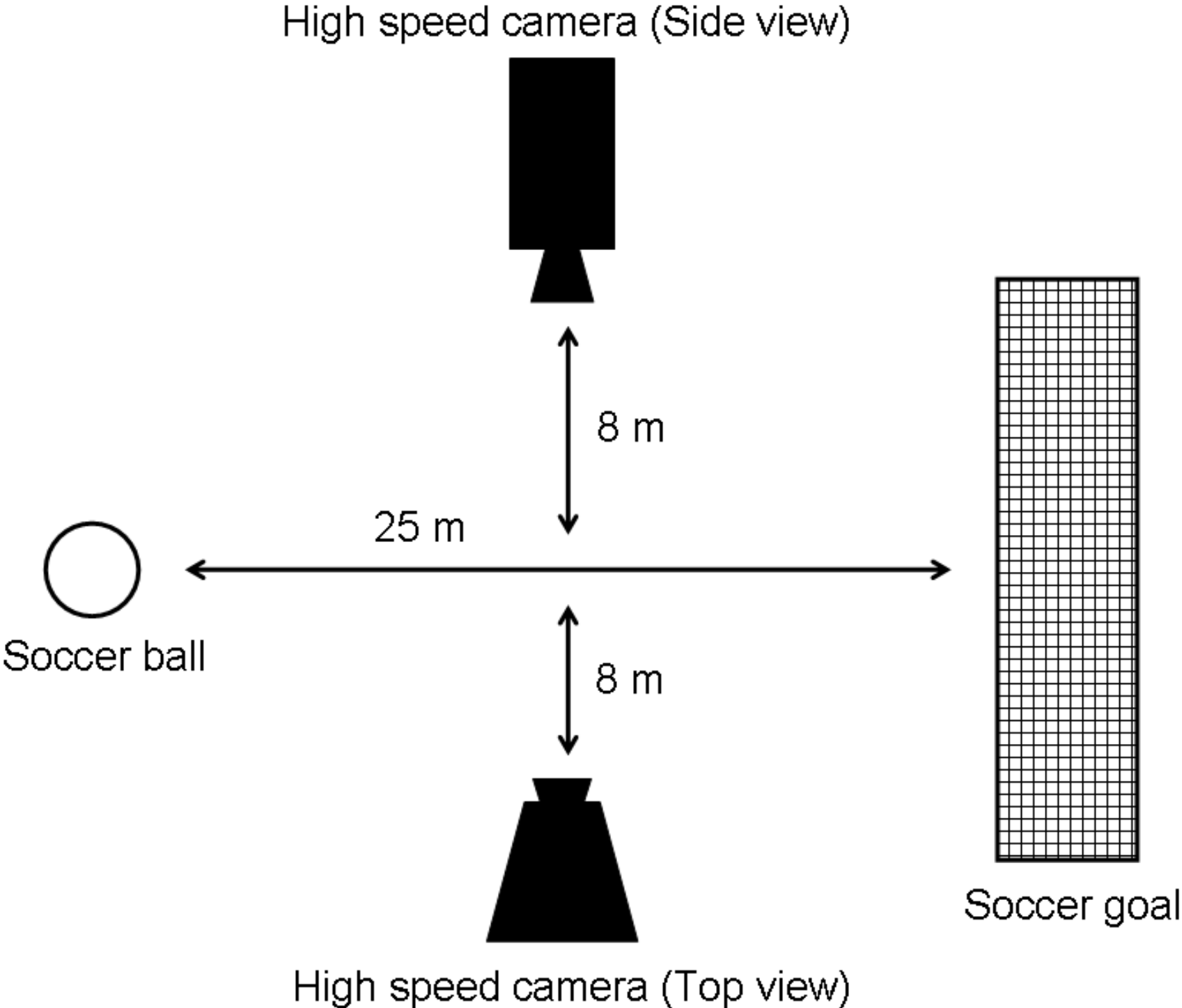
Figure 8. Correlation between frequencies of large-scale vortex trail undulations and acting force in this experiment ($r = 0.94, p < 0.01$).

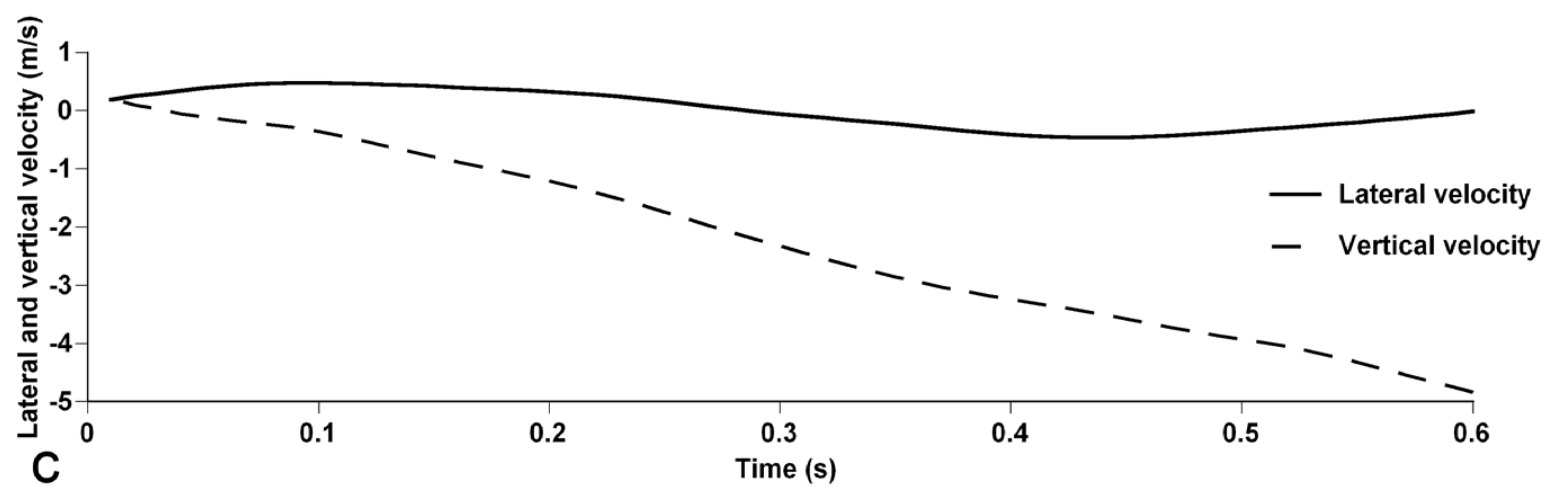
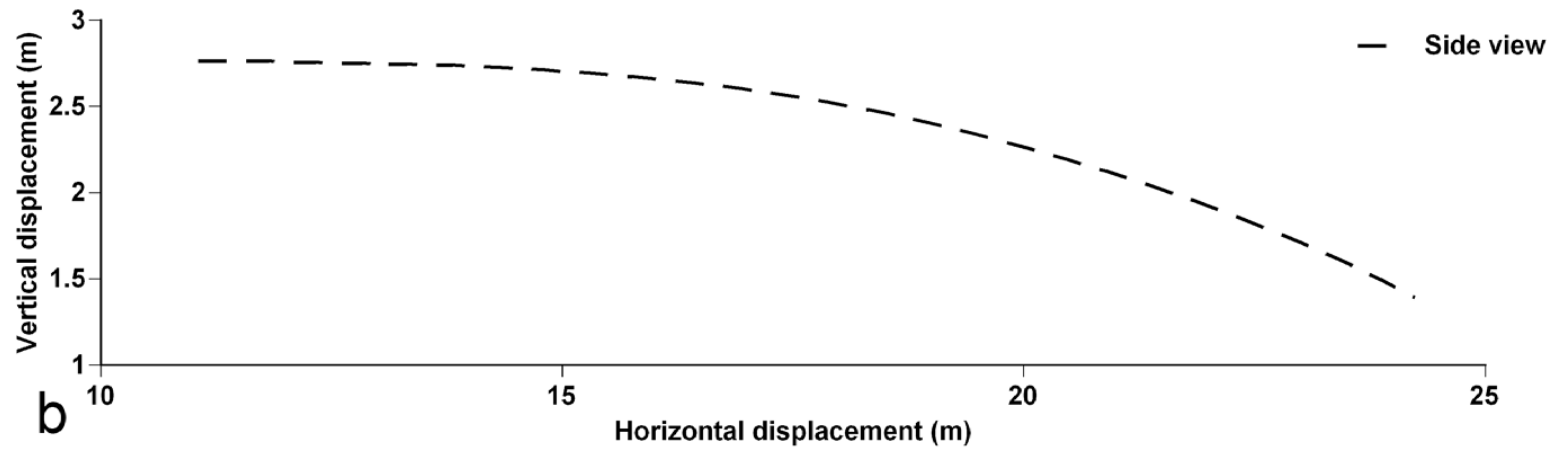
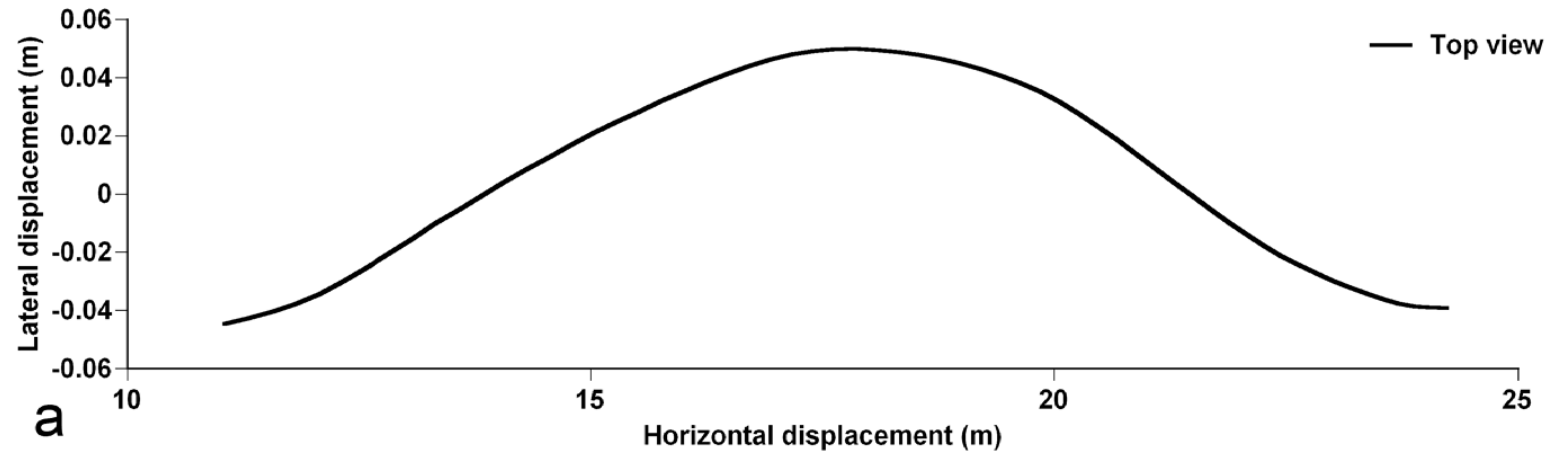
Table 1 The frequency of the fluctuation of lift and side force, the frequency of wake oscillation (Vortex), and the rotation rate of the ball (Rotation).

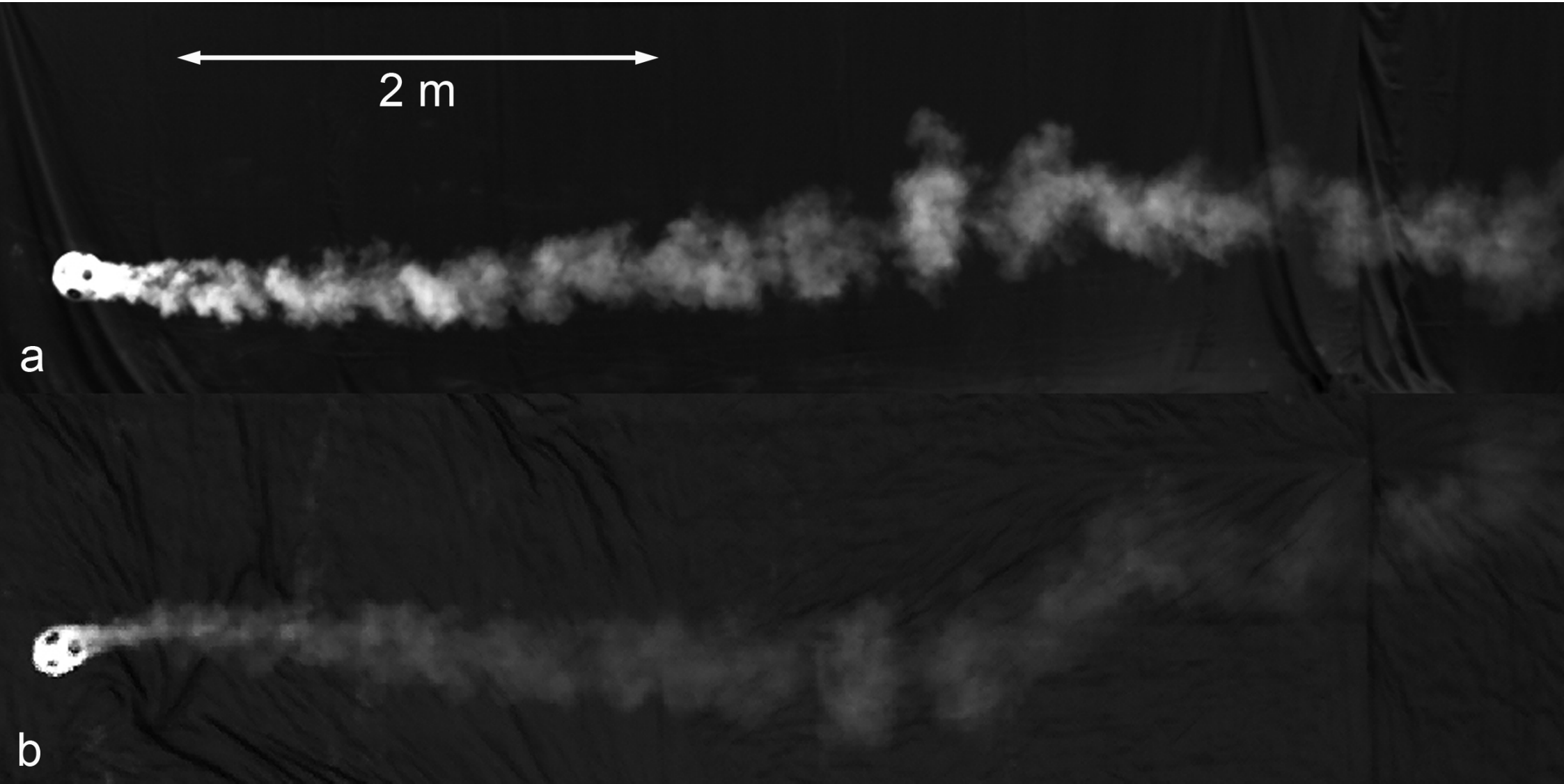
Trial	Lift force (Hz)	Side force (Hz)	Vortex (vertical) (Hz)	Vortex (lateral) (Hz)	Rotation (top spin) (rev. / s)	Rotation (side spin) (rev. / s)
a	7.9	5.7	11.1	5.0	1.3	1.6
b	5.4	2.8	5.0	2.6	0.9	1.4
c	3.4	5.3	3.1	7.1	1.7	1.0
d	2.2	6.3	2.3	6.3	1.9	1.9
e	2.9	3.1	2.3	3.1	1.8	1.3
f	3.7	4.2	3.8	4.2	1.3	0.9
g	3.6	5.4	3.3	5.3	1.4	1.2
h	1.9	2.1	1.9	2.1	0.5	0.6
i	4.8	2.8	5.0	2.4	1.5	0.3
j	4.1	3.7	4.5	3.6	1.3	0.3
mean	4.0	4.1	4.2	4.2	1.4	1.1
s.d.	1.7	1.5	2.7	1.7	0.4	0.5

fig.1









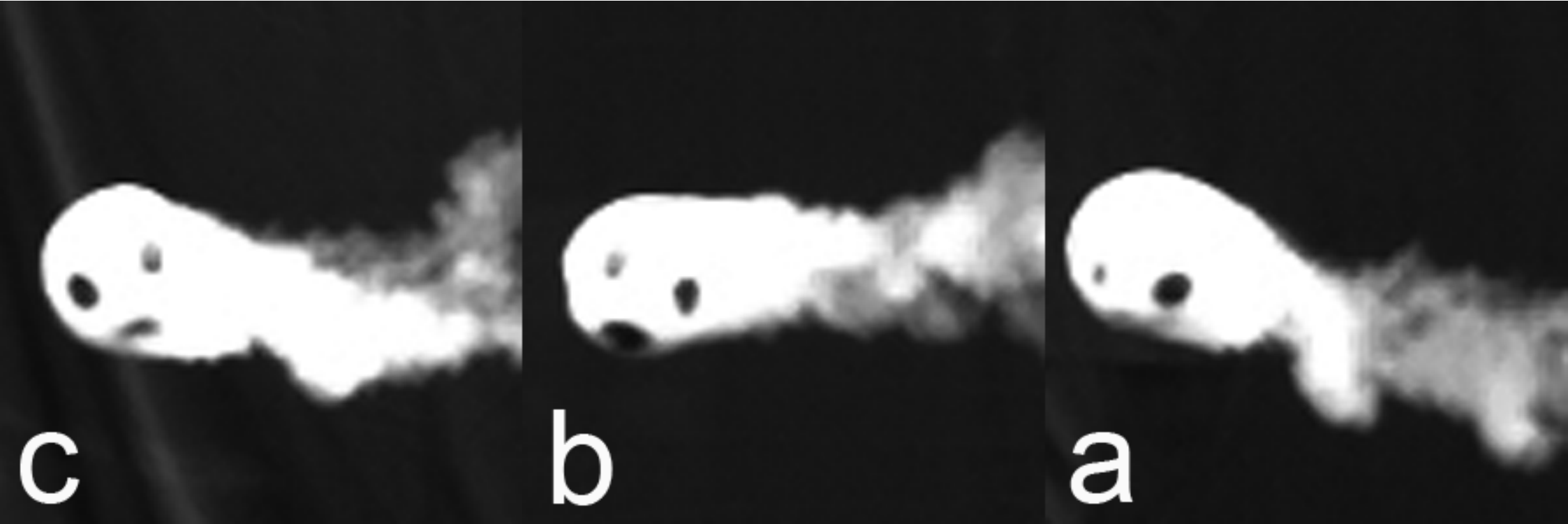


fig.6

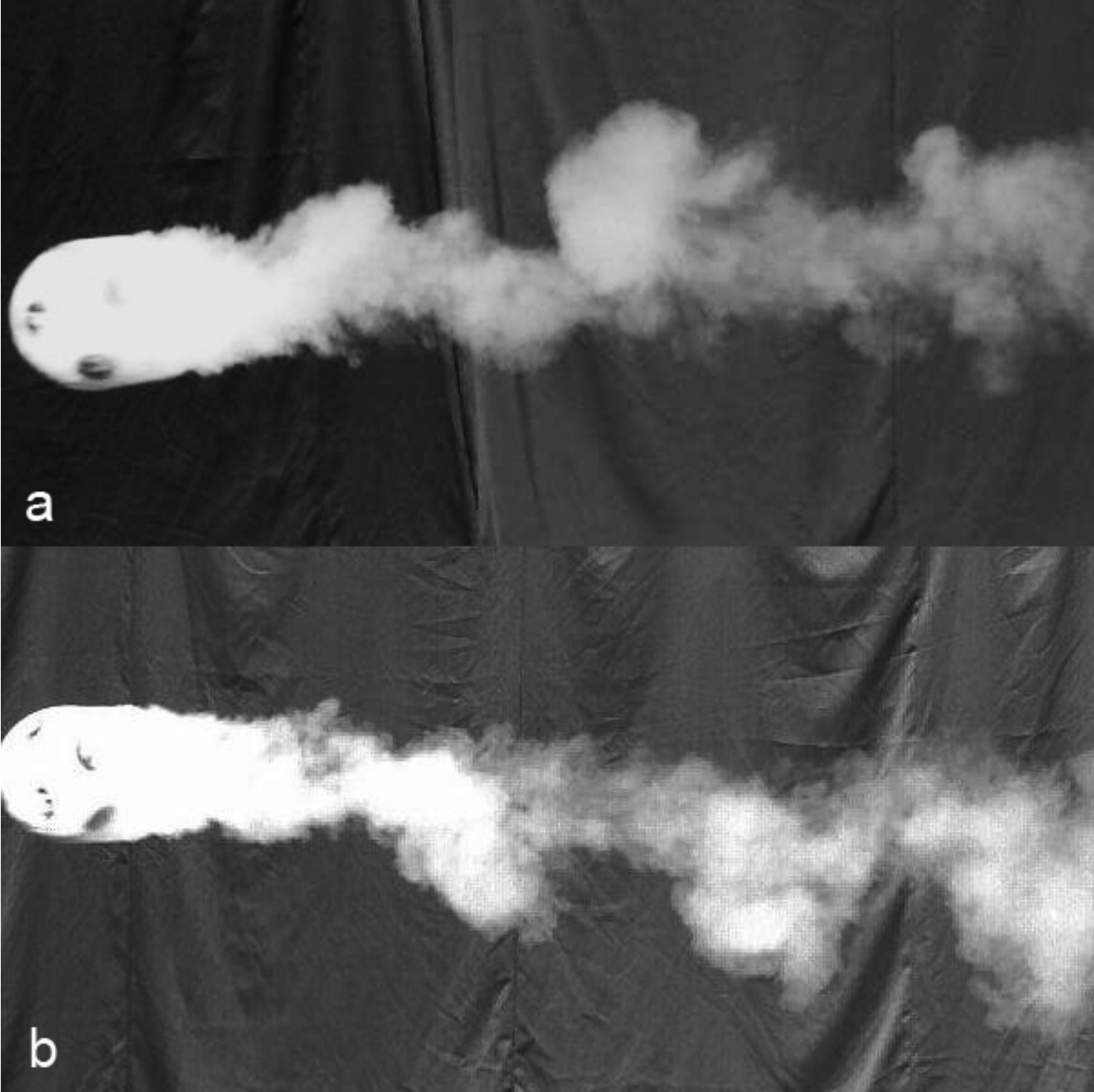


fig.7

